



저작자표시-비영리-변경금지 2.0 대한민국

이용자는 아래의 조건을 따르는 경우에 한하여 자유롭게

- 이 저작물을 복제, 배포, 전송, 전시, 공연 및 방송할 수 있습니다.

다음과 같은 조건을 따라야 합니다:



저작자표시. 귀하는 원저작자를 표시하여야 합니다.



비영리. 귀하는 이 저작물을 영리 목적으로 이용할 수 없습니다.



변경금지. 귀하는 이 저작물을 개작, 변형 또는 가공할 수 없습니다.

- 귀하는, 이 저작물의 재이용이나 배포의 경우, 이 저작물에 적용된 이용허락조건을 명확하게 나타내어야 합니다.
- 저작권자로부터 별도의 허가를 받으면 이러한 조건들은 적용되지 않습니다.

저작권법에 따른 이용자의 권리는 위의 내용에 의하여 영향을 받지 않습니다.

이것은 [이용허락규약\(Legal Code\)](#)을 이해하기 쉽게 요약한 것입니다.

[Disclaimer](#)

Thesis for the Degree of Master of Science

**Characteristics of Wind Speeds and Air  
Temperatures Predicted by the LDAPS:  
Classification by the Types of Land  
Cover and Topography**

by

Dong-Ju Kim

Department of Environmental Atmospheric Sciences

The Graduate school

Pukyong National University

February 2019

Characteristics of Wind Speeds and Air  
Temperatures Predicted by the LDAPS:  
Classification by the Types of Land Cover  
and Topography

(국지예보시스템의 풍속과 기온 예측  
특성: 토지 피복과 지형 유형별 분류)

Advisor: Prof. Jae-Jin Kim  
(Co-Advisor: Prof. Won-Sik Choi)

by

Dong-Ju Kim

A thesis submitted in partial fulfillment of the requirements  
for the degree of

Master of Science

in Department of Environmental Atmospheric Sciences,  
The Graduate School,  
Pukyong National University

February 2019

Characteristics of Wind Speeds and Air Temperatures Predicted  
by the LDAPS: Classification by the Types of Land Cover and  
Topography

A dissertation

by

Dong-Ju Kim

Approved by:



---

(Chairman) Baek-Min Kim



---

(Member) Won-Sik Choi



---

(Member) Jae-Jin Kim

February 22, 2019

# Contents

List of Figures .....	ii
List of Tables .....	v
Abstract .....	vi
1. Introduction .....	1
2. Methodology .....	4
2.1. Points classification and selection .....	4
2.2. Data output and statistical analysis .....	8
3. Results .....	11
3.1. Analysis of 4 category averaged Bias .....	11
3.2. Analysis of the each category LDAPS prediction characteristics ..	14
3.3. Confirmation of prediction characteristics .....	28
4. Summary & Conclusions .....	33
REFERENCE .....	35

# List of Figures

- Fig. 1.** AWS locations selected according to four classification criteria. .... 7
- Fig. 2.** Box Plots for the four categories of (a) averaged wind speed bias and (b) averaged temperature biases. Upper and lower black circles indicate the outliers, the bars above and below the boxes indicate the upper and lower extremes, respectively, and upper, middle, and lower segments of boxes indicate the upper quartiles, medians, and lower quartiles, respectively. The red line represents the mean value of each category biases. .... 13
- Fig. 3.** Bar graph for the wind speeds and air temperatures Bias at (a) Uf type 25 AWS points (b) installed on the ground level (0 m and 1 m). The x-axis represents observation height (m) of AWS. Blue bar represents for wind speeds and red bar represents for air temperatures. .... 16
- Fig. 4.** Correlation diagram between AWS data and LDAPS for AWS points representing Uf types on (a) air temperatures and (b) wind speeds, at AWS 403 (installed on the roof of the building). [(c) and (d)] are same as [(a) and (b)], but at AWS 410 (installed on the ground level). Red dot represents for summer season (June to August), and blue dot represents for winter season (December to February). .... 17
- Fig. 5.** Bar graph for the wind speeds and air temperatures Bias at 25 AWS points on Rf type. The x-axis represents the difference in terrain altitude between the LDAPS and AWS points (m). Blue bar represents for wind speeds and red

bar represents for air temperatures. .... 19

**Fig. 6.** Correlation diagram between AWS data and LDAPS for AWS points representing Rf types on (a) air temperature and (b) wind speed, at AWS 615 (located on a flat area). [(c) and (d)] are same as [(a) and (b)], but at AWS 900 (located on a basin area). Red dot represents for summer season (June to August), and blue dot represents for winter season (December to February). .... 20

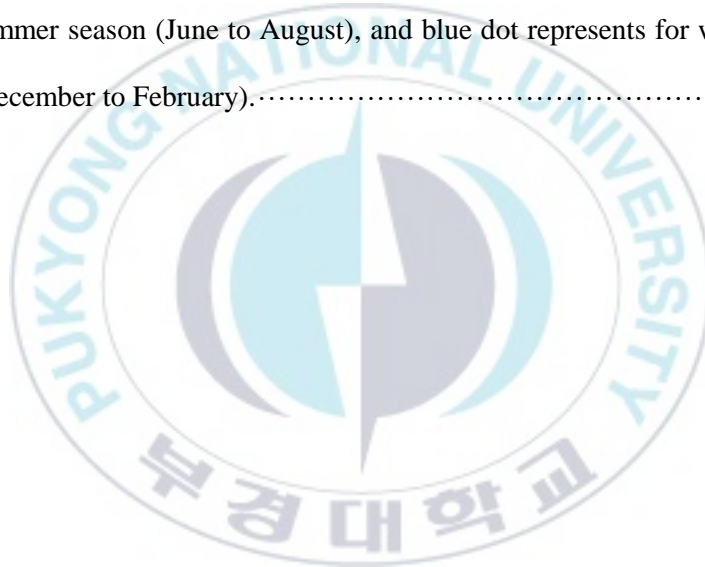
**Fig. 7.** Bar graph for the wind speed and air temperature Biases at 25 AWS points on Rm type. The x-axis represents the difference in terrain altitude between the LDAPS and AWS points (m). Left panel shaded on red color represents the case of LDAPS topographical altitude higher than actual observation altitude. Right shaded panel in blue indicates the opposite case. Blue bar represents for wind speeds and red bar represents for air temperatures. .... 23

**Fig. 8.** Correlation diagram between AWS data and LDAPS for AWS points representing Rm types on (a) air temperature and (b) wind speed, at AWS 316 (LDAPS topographical altitude lower than actual observation altitude). [(c) and (d)] are same as [(a) and (b)], but at AWS 872 (LDAPS topographical altitude higher than actual observation altitude). Red dot represents for summer season (June to August), and blue dot represents for winter season (December to February). .... 24

**Fig. 9.** Box plots for the wind speeds and air temperatures Bias at 25 AWS points on Rc type. Left panel shaded on blue color represents the case of LDAPS grid

located on sea. Right panel shaded on red color represents the case of LDAPS grid located on land. Blue box represents for wind speeds and pink box represents for air temperatures.....26

**Fig. 10.** Correlation diagram between AWS data and LDAPS for AWS points representing Rc types on (a) air temperature and (b) wind speed, at AWS 607 (LDAPS grid located on sea). [(c) and (d)] are same as [(a) and (b)], but at AWS 793 (LDAPS grid located on land). Red dot represents for summer season (June to August), and blue dot represents for winter season (December to February).....27



# List of Tables

**Table 1.** Classification criteria according to land covers and topographies. .... 6

**Table 2.** Information of 100 AWS points. .... 10

**Table 3.** Information of additional 100 AWS points. .... 30



# 국지예보시스템의 풍속과 기온 예측 특성: 토지 피복과 지형 유형별 분류

김동주

부경대학교 대학원 환경대기학과

## 요 약

본 연구는 국지예측시스템(LDAPS)의 토지피복과 지형에 따른 풍속과 기온에 대한 예측 특성을 분석하기 위하여, 기상청 AWS 지점을 2가지 토지피복(도시, 교외)과 3가지 지형(산악, 해안, 평지)에 따라 구분하였다. 표본이 적은 2가지 유형(도시-산악, 도시-해안)을 제외한 4가지 유형에 대하여 각 25개 지점씩 100개 지점에 대하여 과거 1년(2015.1.1~2015.12.31) 동안의 AWS 관측자료와 LDAPS 자료를 이용해 Bias와  $R^2$  값을 계산하여 통계 분석을 수행하였다. 도시-평지 유형의 경우, LDAPS 해상도의 한계로 밀집된 고층 건물과 토지피복에 의한 차등가열의 효과를 제대로 고려하지 못하여 풍속은 과대 모의하고, 기온은 과소 모의하는 패턴이 나타났다. 교외-평지 유형의 경우, 도시 지역에 비해 관측지점 주변으로 장애물이 적어 도시-평지 유형에 비하여 풍속과 기온에 대한 예측 성능이 높은 것으로 나타났다. 교외-산악 유형은, LDAPS 모델의 지형고도와 실제 지형고도간의 차이에 의해 예측 성능이 상이하게 나타났는데, 모델고도가 실제고도보다 높은 경우 풍속을 과대 모의하고 기온을 과소 모의했으며, 모델고도가 실제고도보다 낮은 경우 반대 패턴을 나타냈다. 교외-해안 유형에서는 모든 지점에서 풍속을 과대 모의하였고 특히, LDAPS 격자점이 해안에 위치하는 경우 보다 과대 모의하였다. 기온은 겨울철에 과대 모의하고 여름철에 과소 모의하는 패턴이 나타났다. 추가로 100개 지점의 AWS를 무작위 선정하여 같은 방식으로 분석한 결과, 수치적으로 근소한 차이는 나타났지만, 각 유형에서의 예측 특성을 따르는 것으로 나타났다.

# 1. Introduction

Weather is directly or indirectly associated with daily life and economic activity. Severe weathers often cause disasters claiming human lives and incurring losses of properties (Lesk et al., 2016). However, accurate and precise weather prediction not only helps reduce such disasters but also provides useful information for socio-economic and cultural fields (i.g., agriculture, construction industry, manufacturing industry, distribution industry, energy industry, transportation, tourism, and leisure. In Korea, the demand on the customized weather information has increased in industrial activities (Song, 2014) and on-site weather forecast helped successfully host the 2018 Pyeong-Chang Winter Olympics by providing the weather information in which meteorological caprice is reflected in real time.

The Korea Meteorological Administration (KMA) is conducting weather forecasts using various numerical models to provide quick and high quality weather information. The local data assimilation and prediction system (LDAPS) based on the unified model (UM) of the United Kingdom has been improved to meet the Korean circumstances and it is being used as the operational forecast model. The LDAPS is a high-resolution model with a horizontal resolution of 1.5 km and 70 vertical layers and it covers over the

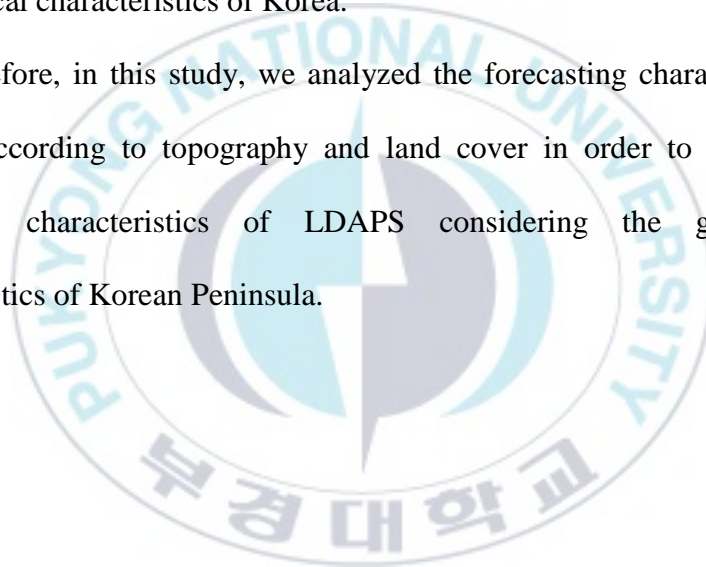
entire Korean peninsula. The LDAPS is designed to resolve small atmospheric phenomena, aiming to prepare for weather disasters caused by local and temporal severe weathers.

Nevertheless, the spatial and temporal resolution of the LDAPS is not high enough to resolve small obstacles such as buildings and hill-like terrain that act as external forcing in or less than urban-scale flows. In addition, it is difficult to consider the effects of temporally and spatially uneven radiative heating and cooling of land surfaces on the air temperature distributions (Park et al., 2016). The temporally and spatially high resolution of the weather forecasting model, LDAPS, enables smaller-scale numerical simulations within the atmospheric boundary layer by providing more realistic initial and boundary conditions to the numerical models with more fine resolution (i.e., computational fluid dynamics model) (Lee and Chun, 2015; Kim et al., 2016; Park et al., 2017). For the application of the LDAPS to multi-scale numerical simulations, need to grasp the characteristics of the meteorological factors predicted by the LDAPS in advance.

Some studies have been conducted to analyze the characteristics of the LDAPS and to improve the prediction performance. Kang et al. (2015) compared the air temperature, wind speed, and relative humidity observed at the Daegu and Gumi meteorological stations for 7 days with those predicted

by the LDAPS, in order to investigate how sensitive the LDAPS prediction is to the initial condition. Yi et al. (2018) showed that the building-scale resolved air temperature (BRT) model improved the performance of the air temperature prediction of the LDAPS by reflecting the heating effect in urban areas. Although previous studies have contributed to the understanding of LDAPS predictive characteristics, there is a lack of research considering the geographical characteristics of Korea.

Therefore, in this study, we analyzed the forecasting characteristics of LDAPS according to topography and land cover in order to analyze the prediction characteristics of LDAPS considering the geographical characteristics of Korean Peninsula.



## 2. Methodology

### 2.1. Points classification and selection

In this study, the automatic weather system (AWS) points of the Korea Meteorological Administration (KMA) were classified according to land covers and topographies. Analyzes land cover (same size as one LDAPS grid) of 1.5km x 1.5km around AWS observation point using 1: 25,000 land cover map provided by EGIS of Ministry of Environment (EGIS). If the ratio of urbanization and dry area was more than 50%, it classified to urban, and to rural less than 50% (Kwon and Lee, 2003). And the topography around the observation point was analyzed and classified into three types according to the terrain characteristics: mountain, coast, flat. When the relief and altitude in the area of 1 km x 1 km around the observation point is more than 200 m, it was classified as mountain (Sung, 2003). If the observation point is within 500 m of the coastal waterside boundary, it was classified as coast (Lee and Kim, 2007). And the areas not belonging to mountainous and coastal terrain were classified as flat. AWS sites were classified into six categories (Um, Uc, Uf, Rm, Rc, Rf) according to land covers and

topographies (Table 1). In this study, 25 points were selected for each of 4 categories (Uf, Rm, Rc, Rf) respectively. Uc and Um types were excluded from the analysis, because of there were few samples where the land cover was classified as urban and the topographies belonged to mountain and coast.



Land use Topography	<b>U</b> <b>(urban)</b>	<b>R</b> <b>(rural)</b>
<b>m</b> <b>(mountain)</b>	<b>Um</b>	<b>Rm</b>
<b>c</b> <b>(coast)</b>	<b>Uc</b>	<b>Rc</b>
<b>f</b> <b>(flat)</b>	<b>Uf</b>	<b>Rf</b>

Table 1. Classification criteria according to land covers and topographies.

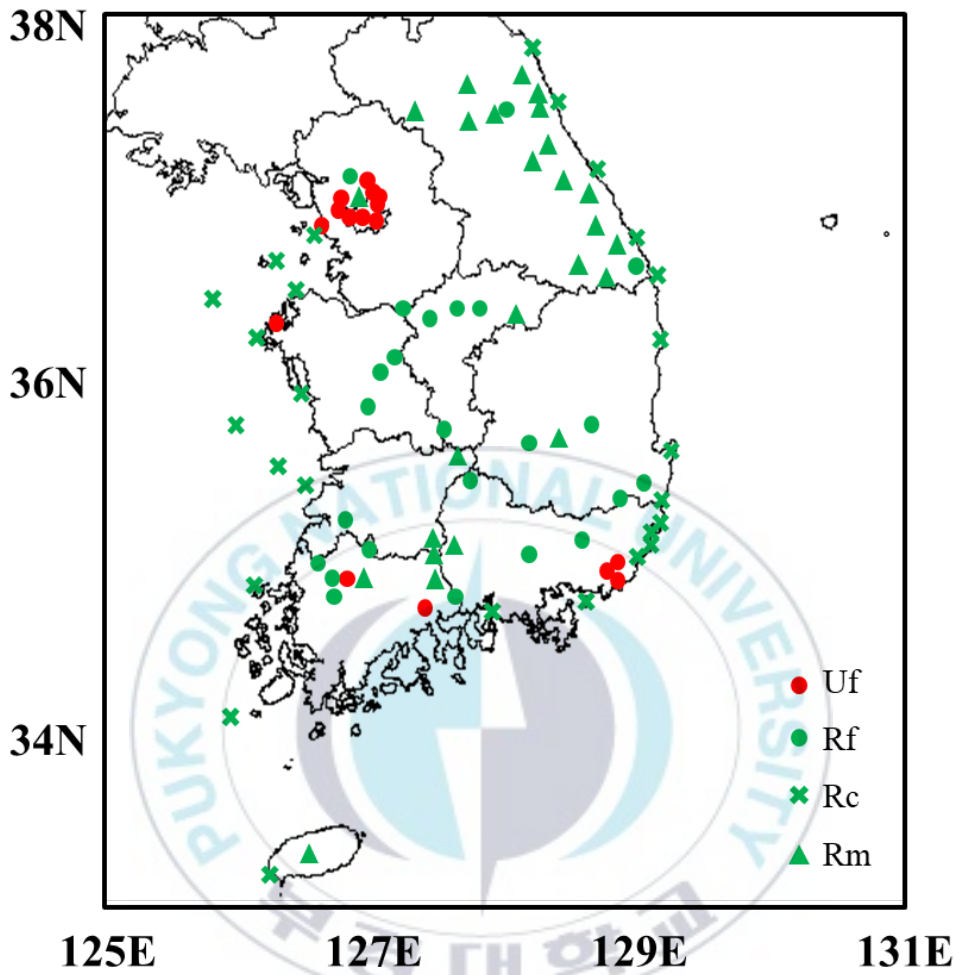


Fig. 1. AWS locations selected according to four classification criteria.

## 2.2. Data output and statistical analysis

The local data assimilation and prediction system (LDAPS) used in this study is the LDAPS-etas (which is model plane) data. LDAPS adopts a resolution of 1.5 km horizontally and performs approximately 40 km of predictions up to 70 levels vertically. It provides analytic fields in 3 hour intervals and provides 36 hour prediction fields (at 00, 06, 12, 18 UTC) and 3 hour prediction fields (at 03, 09, 15, 21 UTC). In this study, using the 1 - hour interval LDAPS data, which is 3 - hour interval analysis field and the 2 - hour prediction field at each analysis time. The u, v, and pot values at the closest LDAPS grid to the each AWS points were calculated, and calculated the 10 m wind speeds and 1.5 m air temperatures by interpolating and extrapolating it to the observation altitude.

Statistical analysis was conducted using AWS observation data and LDAPS prediction data for 1 year (2015.1.1 ~ 2015.12.31). Analyzed the predictive characteristics of LDAPS using mean deviation (Bias) and analyzed the correlation with observation data using the coefficient of determination ( $R^2$ ). Bias and  $R^2$  were calculated using the following equation.

$$\text{Bias} = \frac{1}{n} (\sum_1^i M_i - O_i) \quad (1)$$

$$R^2 = \left( \frac{(M_i - \bar{M}_i)(O_i - \bar{O}_i)}{\sigma_{M_i}\sigma_{O_i}} \right)^2 \quad (2)$$

Where,  $M_i$  is the i-th LDAPS predicted values,  $O_i$  is the i-th observed values,  $n$  is the total number of data,  $\sigma_{M_i}$  is the LDAPS deviation, and  $\sigma_{O_i}$  is the AWS deviation, respectively. The value of Bias,  $R^2$ , altitude, and classification type information at each AWS points were shown in Table 2.



Station number	Difference of altitude	Category	Bias (wind speeds/temperature)	R <sup>2</sup> (wind speeds/temperature)	Station number	Difference of altitude	Category	Bias (wind speeds/temperature)	R <sup>2</sup> (wind speeds/temperature)
300	48.00	Rc	0.04 / -1.35	0.55 / 0.72	662	13.53	Rc	1.70 / -1.19	0.48 / 0.73
301	4.40	Rc	1.53 / -1.49	0.64 / 0.69	663	60.48	Rc	0.32 / -0.87	0.60 / 0.82
310	-80.22	Rc	1.25 / -0.25	0.34 / 0.67	671	1.40	Rc	1.39 / -1.81	0.27 / 0.49
316	501.53	Rm	-2.38 / 3.47	0.08 / 0.85	682	558.78	Rm	-1.06 / 3.07	0.01 / 0.72
318	-33.41	Rm	0.93 / 0.54	0.58 / 0.73	695	463.78	Rm	-1.53 / 2.52	0.05 / 0.86
320	347.84	Rm	0.23 / 2.32	0.28 / 0.87	697	4.00	Rc	2.07 / -1.45	0.52 / 0.76
321	-190.50	Rf	0.34 / -0.58	0.51 / 0.85	700	52.32	Rc	1.16 / -1.07	0.42 / 0.85
400	34.98	Uf	1.29 / -1.03	0.28 / 0.90	701	-17.10	Rf	0.43 / 0.74	0.30 / 0.85
401	3.97	Uf	1.08 / -1.84	0.45 / 0.89	706	-30.25	Rf	-0.12 / -0.55	0.48 / 0.89
402	-22.20	Uf	1.96 / -1.15	0.26 / 0.93	708	-11.25	Rf	0.60 / -1.05	0.59 / 0.89
403	45.09	Uf	1.92 / -1.91	0.21 / 0.90	710	-31.87	Rf	0.86 / -0.87	0.63 / 0.87
404	59.57	Uf	1.75 / -1.82	0.27 / 0.91	712	-50.06	Uf	0.36 / -1.40	0.56 / 0.91
405	-16.49	Uf	1.15 / -1.91	0.34 / 0.89	735	-16.04	Rm	1.08 / 0.23	0.41 / 0.73
406	-229.35	Uf	1.96 / -2.48	0.21 / 0.87	759	-393.87	Rm	1.58 / -1.22	0.16 / 0.54
408	5.47	Uf	0.96 / -0.73	0.22 / 0.89	775	27.46	Rf	0.33 / -0.94	0.68 / 0.92
409	19.80	Uf	0.63 / -1.32	0.29 / 0.92	788	36.08	Uf	1.02 / -1.36	0.28 / 0.88
410	25.20	Uf	0.65 / -1.27	0.40 / 0.81	791	-386.60	Rm	1.02 / -1.02	0.36 / 0.65
413	10.60	Uf	0.97 / -1.72	0.26 / 0.92	793	-0.53	Rc	0.58 / -1.37	0.66 / 0.91
415	17.27	Uf	1.46 / -1.80	0.19 / 0.89	800	-155.47	Rc	0.96 / -0.09	0.32 / 0.64
416	8.48	Rf	0.64 / -0.03	0.47 / 0.88	816	-37.79	Rf	0.54 / -0.20	0.53 / 0.79
417	22.76	Uf	1.32 / -1.73	0.21 / 0.90	825	-58.35	Rf	0.11 / -1.20	0.45 / 0.86
419	201.73	Rm	0.40 / 0.98	0.20 / 0.84	829	-84.79	Rf	0.38 / -0.27	0.60 / 0.89
421	-17.57	Uf	1.40 / -1.84	0.20 / 0.90	831	-233.41	Rm	2.07 / 0.48	0.37 / 0.59
422	85.67	Rm	0.37 / 0.80	0.24 / 0.92	838	-239.97	Rm	0.95 / -1.94	0.41 / 0.84
423	14.56	Uf	1.08 / -1.13	0.18 / 0.91	841	-117.05	Rf	0.37 / 1.01	0.49 / 0.79
424	-233.04	Uf	1.47 / -1.65	0.31 / 0.94	852	38.47	Rc	0.76 / -1.15	0.56 / 0.83
496	6.22	Rf	0.52 / -0.69	0.41 / 0.89	853	81.92	Rm	1.89 / 0.56	0.21 / 0.91
497	-140.91	Rm	2.68 / 0.95	0.31 / 0.62	856	-218.79	Rm	1.78 / -1.33	0.38 / 0.76
498	206.34	Rm	0.60 / 1.49	0.13 / 0.87	870	40.97	Rm	0.67 / 0.80	0.39 / 0.71
510	11.06	Uf	1.59 / -1.77	0.17 / 0.88	872	-426.02	Rm	1.66 / -2.3	0.21 / 0.62
512	0.71	Uf	1.03 / -1.55	0.25 / 0.83	875	496.67	Rm	-0.92 / 2.95	0.22 / 0.81
524	3.00	Rc	0.46 / -1.87	0.24 / 0.69	878	218.47	Rm	1.06 / 0.87	0.22 / 0.87
529	-130.88	Rf	0.37 / 0.57	0.32 / 0.72	881	13.00	Rc	1.19 / -1.53	0.29 / 0.67
554	-8.22	Rm	-1.69 / 0.62	0.60 / 0.75	887	-26.56	Rf	0.31 / -0.96	0.54 / 0.89
559	-199.97	Rm	0.95 / 0.48	0.52 / 0.76	900	-234.02	Rf	0.62 / -0.56	0.52 / 0.75
572	-41.97	Uf	0.91 / -1.53	0.39 / 0.90	901	34.37	Rc	1.23 / -1.41	0.42 / 0.81
579	-94.66	Rm	0.74 / 0.67	0.41 / 0.78	907	-17.58	Rc	1.40 / -1.49	0.35 / 0.79
581	-185.47	Rm	0.32 / -0.45	0.31 / 0.84	920	-38.16	Rf	0.52 / -0.65	0.54 / 0.89
586	-198.04	Rm	0.97 / -1.11	0.39 / 0.84	921	73.70	Rc	1.54 / -1.21	0.38 / 0.77
602	-44.06	Rf	0.67 / -0.17	0.45 / 0.87	923	20.75	Rc	1.17 / -1.19	0.41 / 0.83
603	-53.51	Rf	0.48 / -0.03	0.52 / 0.88	924	16.40	Rc	1.41 / -1.51	0.36 / 0.81
606	24.00	Rc	1.60 / -1.60	0.48 / 0.75	925	-0.26	Rf	0.51 / -0.82	0.47 / 0.89
607	7.00	Rc	2.00 / -1.67	0.56 / 0.70	932	-23.10	Rf	0.72 / -1.95	0.28 / 0.91
615	11.09	Rf	0.26 / -0.98	0.49 / 0.94	938	-6.97	Uf	0.75 / -0.84	0.35 / 0.80
622	-50.62	Rf	0.54 / 0.06	0.56 / 0.84	940	-171.47	Uf	1.50 / -1.07	0.24 / 0.82
623	-81.71	Rf	0.65 / -0.61	0.50 / 0.90	942	-49.32	Uf	1.72 / -1.26	0.27 / 0.84
627	15.54	Uf	0.82 / -1.08	0.47 / 0.85	946	-176.24	Rf	0.22 / -0.86	0.47 / 0.78
631	9.00	Rc	1.23 / -1.76	0.52 / 0.73	949	-76.55	Rc	0.67 / -1.00	0.39 / 0.72
657	32.00	Rc	1.08 / -1.53	0.33 / 0.71	951	-61.22	Rf	0.35 / 0.50	0.49 / 0.84
661	5.00	Rc	0.06 / -0.86	0.23 / 0.51	954	62.60	Rc	0.91 / -1.61	0.37 / 0.84

**Table 2. Information of 100 AWS points.**

## 3. Results

### 3.1. Analysis of 4 categories averaged Bias

For each of the four categories classified by land covers and topographies, the biases at 25 AWS points for each category were averaged to analyze the predictive characteristics of LDAPS. In the case of wind speed, LDAPS is overestimated as an all compared to observed values. The average of bias was highest in Uf ( $1.25 \text{ m s}^{-1}$ ) and lowest in Rf ( $0.43 \text{ m s}^{-1}$ ). In the Rm type, the average of Bias was  $0.57 \text{ m s}^{-1}$ , which was lower than that of the Uf and Rc types, but the deviation of the point-to-point Bias was largest (Maximum  $2.68 \text{ m s}^{-1}$  / minimum  $-2.38 \text{ m s}^{-1}$ ). In Rc type, the average and deviation of point-to-point Bias were  $1.11 \text{ m s}^{-1}$  and  $0.52 \text{ m s}^{-1}$ , and overestimated at the all points similar to Uf type (Fig. 2a).

In the case of air temperature, the tendency was opposite to the wind speed case. In Uf type, LDAPS has underestimated overall, and the average magnitude of the Bias was highest. In Rf type, unlike the wind speed characteristics, the deviation between the each points was large. In Rm type, the average of Bias was similar to wind speed case, but the deviation

distribution pattern was reversed. The Rc type has the smallest average and deviation of point-to-point Bias among four categories, so it showed that the prediction performance of LDAPS is better than wind speed case (Fig. 2b).



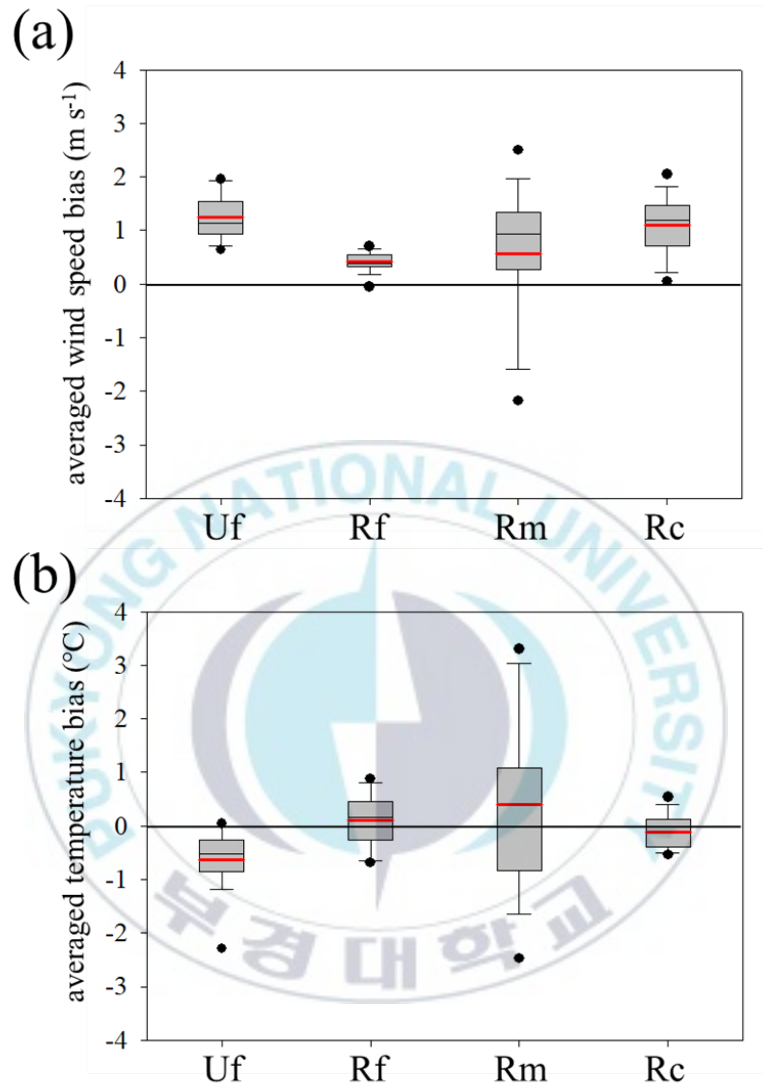


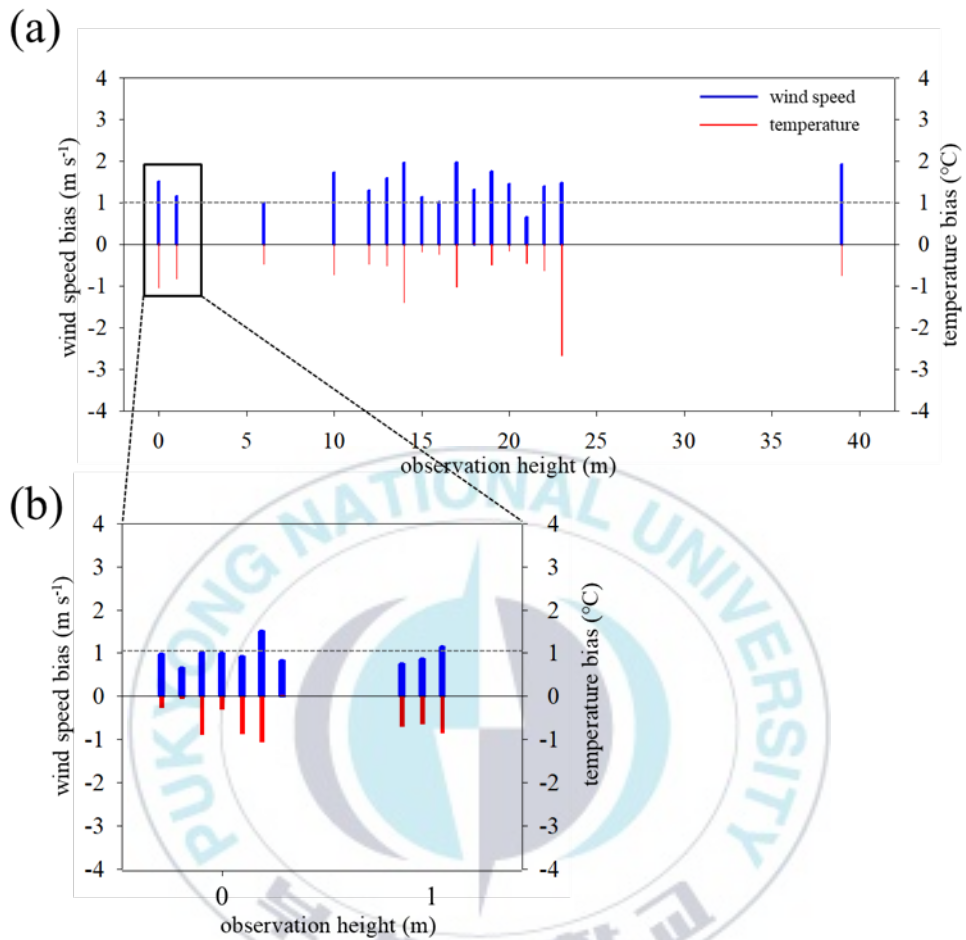
**Fig. 2. Box Plots for the 4 categories of (a) averaged wind speed bias and (b) averaged temperature biases. Upper and lower black circles indicate the outliers, the bars above and below the boxes indicate the upper and lower extremes, respectively, and upper, middle, and lower segments of boxes indicate the upper quartiles, medians, and lower quartiles, respectively. The red line represents the mean value of each category biases.**

### **3.2. Analysis of the each category LDAPS prediction characteristics**

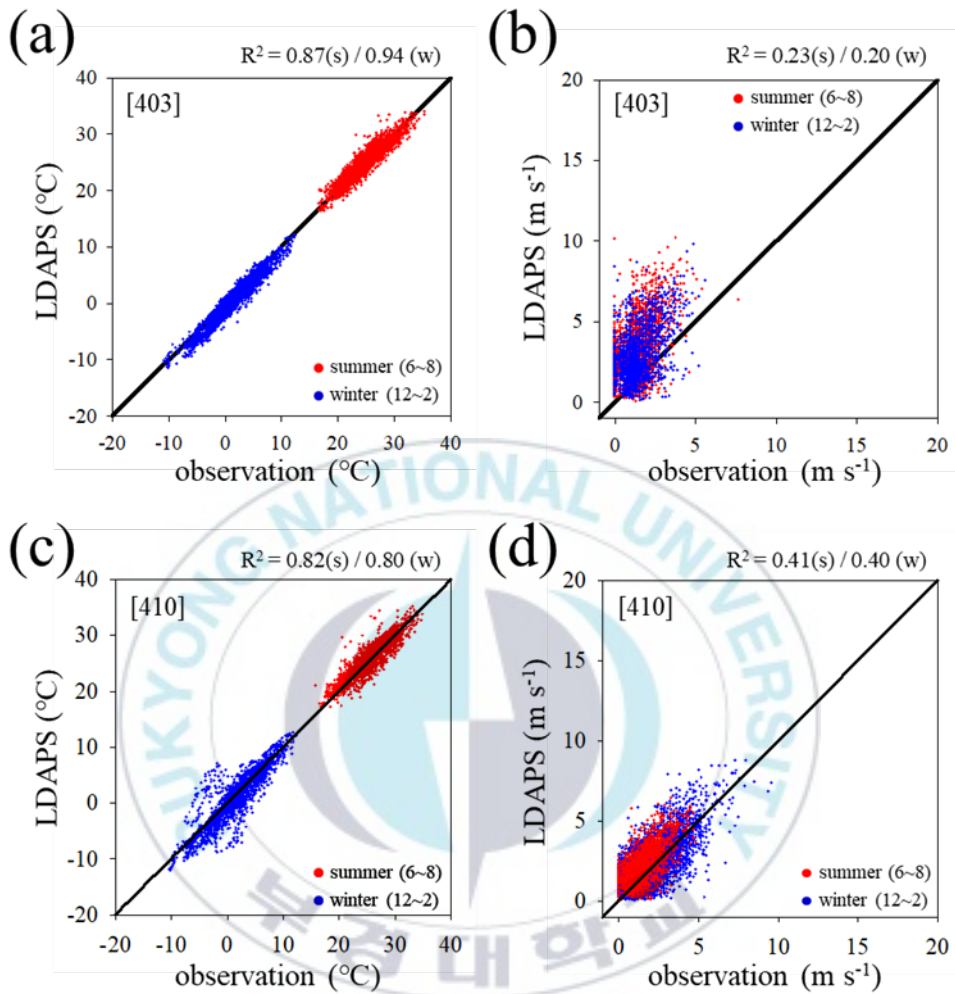
In this section, Bias and  $R^2$  were analyzed for a year at each 25 sites by category, and the characteristics of each category were analyzed in detail. Figure 3 shows the annual average Bias of wind speed and air temperature at 25 Uf stations. In the case of Uf, the wind speed was overestimated at all points and the air temperature was underestimated at all points except the two points (Fig. 3a). Based on the unified model (UM), LDAPS uses the MOSES-II land surface scheme to classify the clusters into nine categories, and apply the urban parametrization through the weighted average of the clusters (Best, 2005). Nevertheless, due to the limitation of the resolution, it showed that the flow change caused by the dense buildings in the urban area and the differential heating effect by the land use type were did not reflect properly. Comparing the differences between the points, the wind speed was overestimated when AWS was installed on the roof of the building, and there was no clear trend for temperature (Fig. 3b). Correlations between AWS data and LDAPS were highly correlated at both on the building-installed points (summer = 0.87, winter = 0.94) and ground-installed points (summer = 0.82, winter = 0.80). In the case of wind speed, the correlation was low on  $R^2 = 0.2$

at the point where the installed on the roof of the building, and  $R^2 = 0.4$  at the point installed on the ground (Fig. 4).



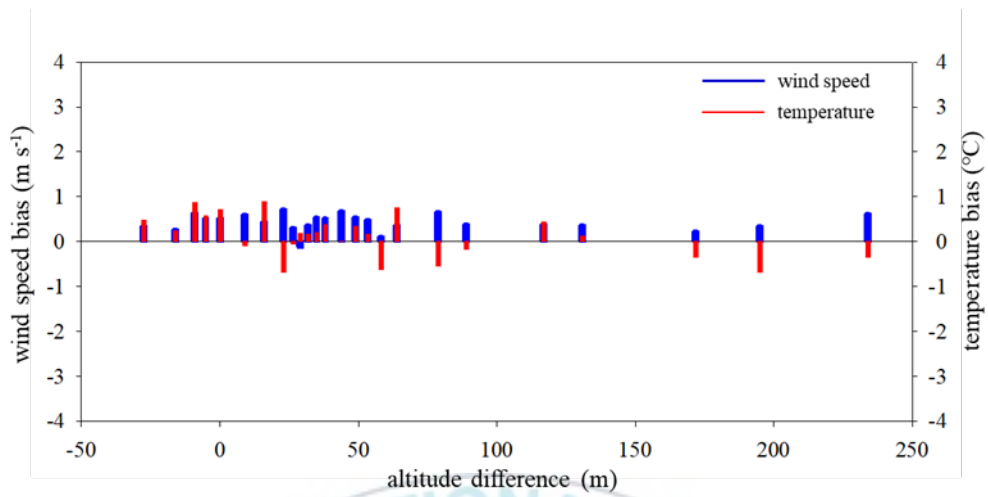


**Fig. 3. Bar graph for the wind speeds and air temperatures Bias at (a) Uf type 25 AWS points (b) installed on the ground level (0 m and 1 m). The x-axis represents observation height (m) of AWS. Blue bar represents for wind speeds and red bar represents for air temperatures.**

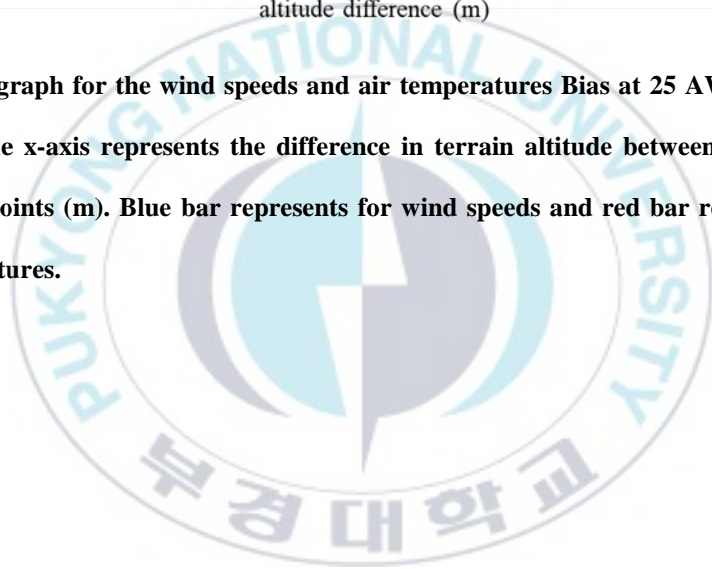


**Fig. 4. Correlation diagram between AWS data and LDAPS for AWS points representing Uf types on (a) air temperatures and (b) wind speeds, at AWS 403 (installed on the roof of the building). [(c) and (d)] are same as [(a) and (b)], but at AWS 410 (installed on the ground level). Red dot represents for summer season (June to August), and blue dot represents for winter season (December to February).**

In case of Rf type, both air temperature and wind speed tend to overestimate overall. The wind speed was overestimated at all points except one point and the air temperature was overestimated at 17 points (Fig. 5). Bias of each point was smaller than Uf type, because it has few obstacles around the observation point, unlike the urban area, and LDAPS seems to simulate the observations well. The average of Bias at 25 points for wind speed and temperature were 0.43 and -0.39, respectively, which were smaller than those of Uf type. The correlation between the AWS data and the LDAPS predicted temperature was very high at  $R^2 = 0.93$  at the point where the flat area, and the wind speed was 0.5, and showed a relatively higher correlation than with Uf type (Figs. 6a and b). In case of the terrain representing the basin type, the LDAPS terrain altitude is higher than the actual altitude. As a result, predictive performance of LDAPS is lower than flat terrain case (Figs. 6c and d). Unlike in Uf type, Rf type has a relatively high prediction performance of LDAPS because it does not have the effect of flow distortion caused by the building, and the heating effect by the land cover. And there was not a clear tendency between the each point.



**Fig. 5. Bar graph for the wind speeds and air temperatures Bias at 25 AWS points on Rf type. The x-axis represents the difference in terrain altitude between the LDAPS and AWS points (m). Blue bar represents for wind speeds and red bar represents for air temperatures.**



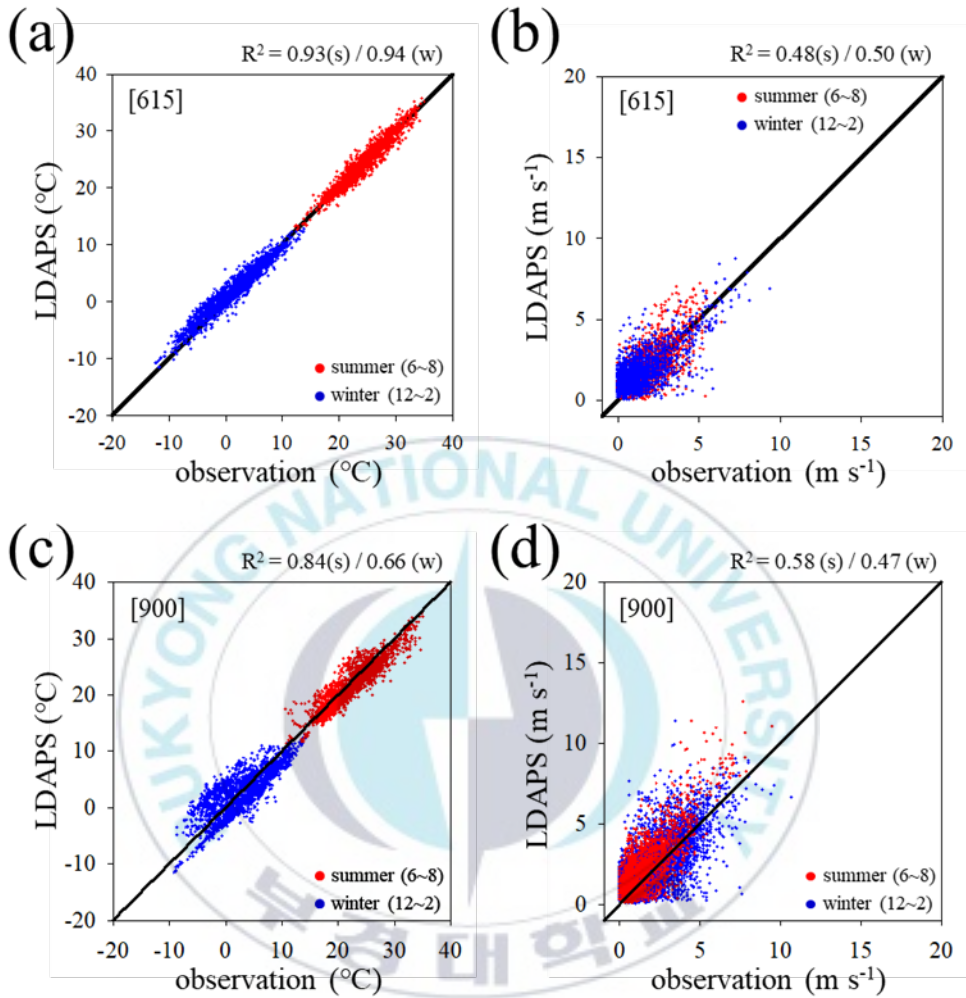


**Fig. 6. Correlation diagram between AWS data and LDAPS for AWS points representing Rf types on (a) air temperature and (b) wind speed, at AWS 615 (located on a flat area). [(c) and (d)] are same as [(a) and (b)], but at AWS 900 (located on a basin area). Red dot represents for summer season (June to August), and blue dot represents for winter season (December to February).**

In the case of Rm, the Bias deviation between each point both wind speed and air temperature was the largest among the four categories (Fig. 2). The wind speed and air temperature predicted characteristics of LDAPS showed the opposite tendency. The larger difference between the LDAPS topographical altitude and the actual terrain altitude, the larger the deviation (Fig. 7). This is a result of smoothing the terrain because the problem of model running occurs when the slope of the terrain in the numerical model is severe (Lim et al., 2011). When the observation point is located at the mountain peaks or ridges higher than surrounding area, the LDAPS topographical altitude is calculated to be lower than the actual altitude, and there is a pattern of underestimating the wind speed and overestimating the air temperature. On the contrary, when the observation point is located in the valley or the basin, the terrain altitude in the model is calculated to be higher than the actual altitude, and the opposite pattern appears. Where the terrain elevation is higher than the actual altitude (such as AWS 316), the  $R^2$  value of the temperature is 0.81 in summer and 0.89 in winter, indicating a high correlation between observed and LDAPS data. However, the wind speed was 0.1 or less irrespective of the season, indicating that there was little correlation between the two data. Conversely, the point where the terrain altitude in LDAPS is calculated to be lower than the actual altitude (such as

AWS 872) showed a relatively high correlation with  $R^2 = 0.6$  at the air temperature, but the correlation was very low at  $R^2 = 0.2$ .



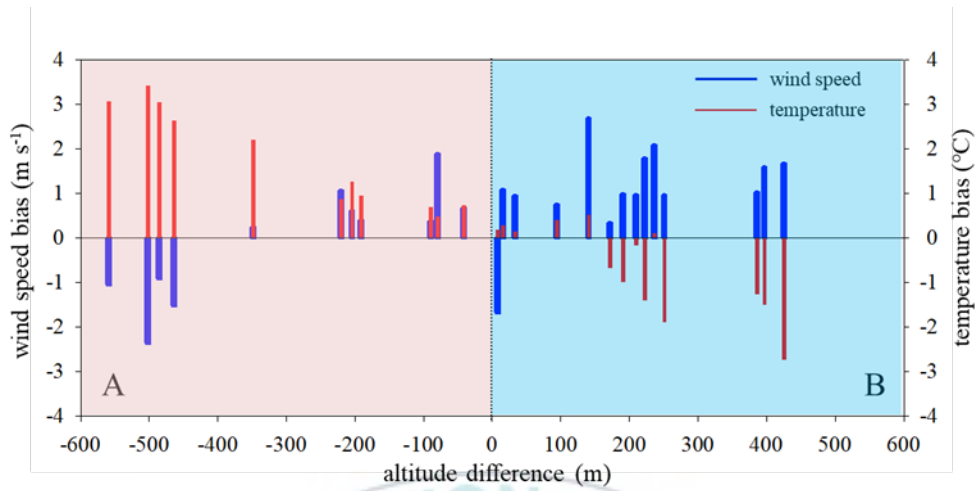


**Fig. 7.** Bar graph for the wind speed and air temperature Biases at 25 AWS points on Rm type. The x-axis represents the difference in terrain altitude between the LDAPS and AWS points (m). Left panel shaded on red color represents the case of LDAPS topographical altitude higher than actual observation altitude. Right shaded panel in blue indicates the opposite case. Blue bar represents for wind speeds and red bar represents for air temperatures.

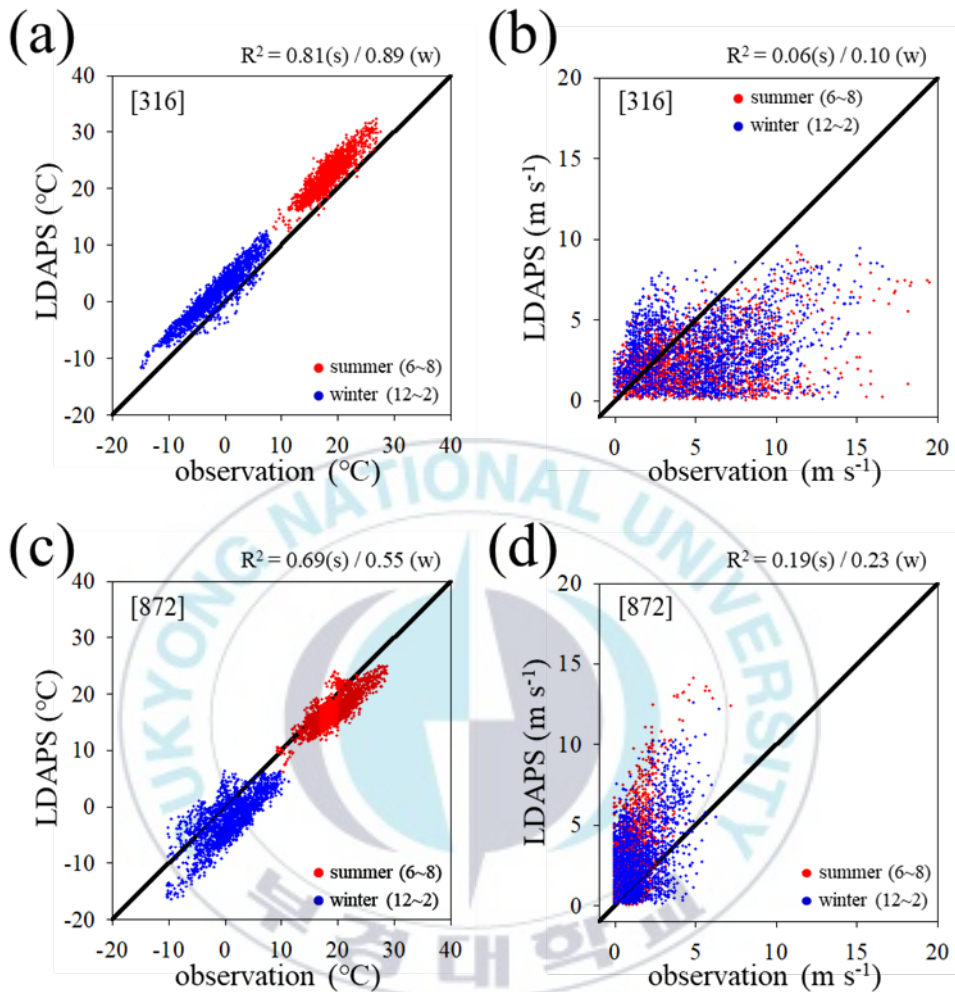


**Fig. 8.** Correlation diagram between AWS data and LDAPS for AWS points representing Rm types on (a) air temperature and (b) wind speed, at AWS 316 (LDAPS topographical altitude lower than actual observation altitude). [(c) and (d)] are same as [(a) and (b)], but at AWS 872 (LDAPS topographical altitude higher than actual observation altitude). Red dot represents for summer season (June to August), and blue dot represents for winter season (December to February).

In case of Rc, the wind speed was overestimated for all of AWS points. In particular, since the point at which the LDAPS grid is represented by the sea does not reflect the ground characteristics at the actual observation point, it has been shown that the LDAPS grid simulates wind speed more overestimation compared to the point where it appears on land (Fig. 9). This is caused by the property that the surface of the LDAPS is treated as the sea (or land) when there are three or fewer grid points where the characteristics of the eight neighboring grid points around the grid point are classified as land (or sea) (Lim et al., 2011). At the point where the LDAPS grid is calculated to the sea (such as AWS 607), the temperature is overestimated in the winter due to the effect of the specific heat between the land and the coast, and underestimated in the summer (Fig. 10a). Correlation between AWS data and LDAPS indicates that if LDAPS grid was appeared at sea, the air temperature  $R^2 = 0.7$  and the wind speed  $R^2 = 0.55$ , indicating a relatively high correlation between both air temperature and wind speed (Figs. 10a and b). When the LDAPS grid were located on land,  $R^2$  of air temperature and wind speed were 0.91 and 0.65, respectively, showed higher correlation than those appear on sea (Figs. 10c and d). It seems that the result of LDAPS reflecting the surface characteristics of the observation point.

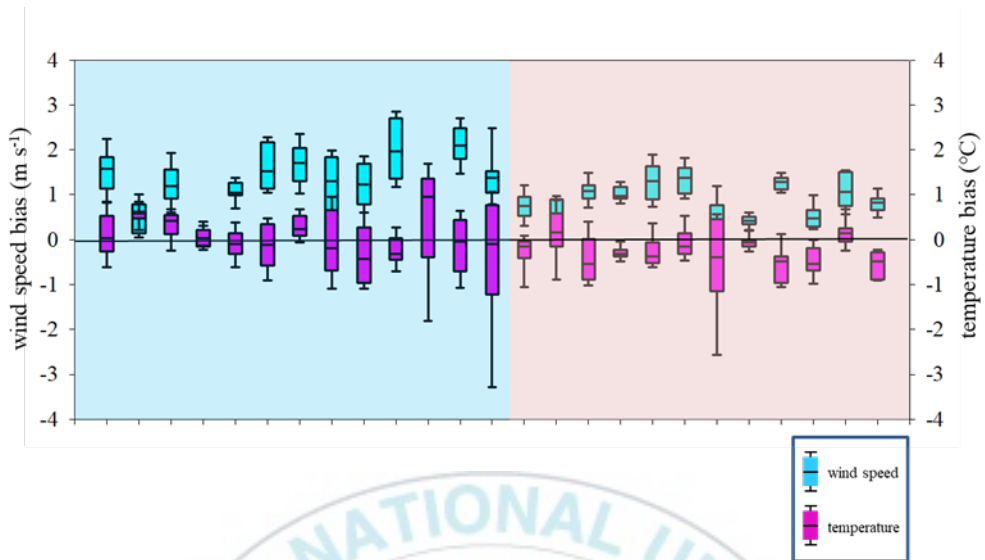


**Fig. 9. Box plots for the wind speeds and air temperatures Bias at 25 AWS points on Rc type. Left panel shaded on blue color represents the case of LDAPS grid located on sea. Right panel shaded on red color represents the case of LDAPS grid located on land. Blue box represents for wind speeds and pink box represents for air temperatures.**

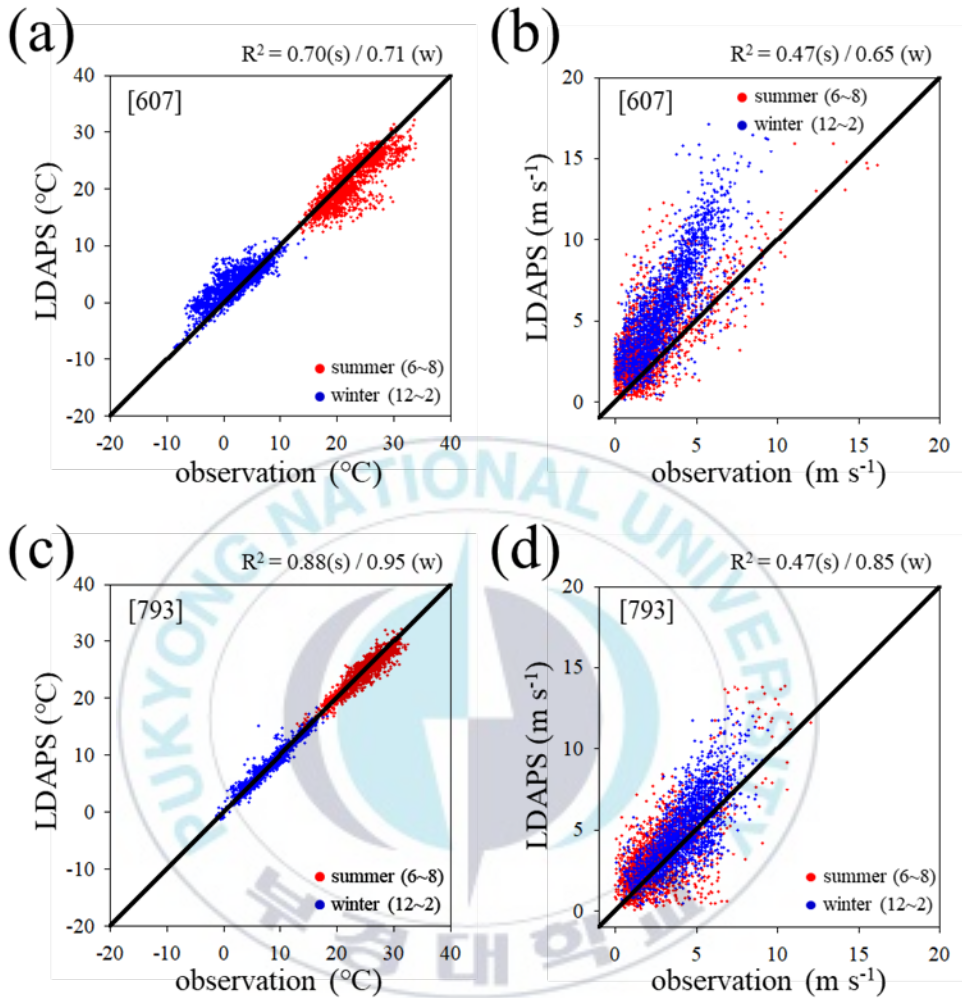


**Fig. 10. Correlation diagram between AWS data and LDAPS for AWS points representing Rc types on (a) air temperature and (b) wind speed, at AWS 607 (LDAPS grid located on sea). [(c) and (d)] are same as [(a) and (b)], but at AWS 793 (LDAPS grid located on land). Red dot represents for summer season (June to August), and blue dot represents for winter season (December to February).**

### 3.3. Confirmation of prediction characteristics

In order to confirm the prediction characteristics of LDAPS analyzed by four categories according to land cover and topographies at AWS points not selected in this study, 100 AWS points were non-restoring extracted using a random function. And then, additional 100 selected AWS points were classified into four categories according to the classification criteria proposed in this study. The information of additional AWS points was represented on Table 3.

The average of wind speed Bias was  $0.71 \text{ m s}^{-1}$  and the average air temperature Bias was  $-0.35^{\circ}\text{C}$  at 19 AWS stations classified as Uf. Compared with the existing Uf type 25 points, the area of the urbanized area including the high-rise buildings was small, so that the wind speed and the air temperature Bias were closer to zero. But there was a pattern of overestimation of the wind speed and underestimation of the temperature, as the overall. In case of the wind speed correlation between AWS data and LDAPS was higher in winter than in summer ( $R^2$  were 0.25 in summer and 0.44 in winter), and the case of air temperature correlation was high ( $R^2=0.88$ ) regardless of the season.

The Rf type that indicating the environment of a general observation point was selected 53 AWS points. Unlike the analysis in Section 3.2, the Rf

type showed large variation in wind speed and air temperature from point to point. This is due to the characteristics of LDAPS (such as basin), as in the Rm type, where the LDAPS topographic altitude is higher than the actual terrain elevation. The average Biases of wind speed and temperature for each point were 0.60 and -0.04, respectively, which were not significantly different from the results shown in Section 3.2, but the deviation between points showed a large difference of 0.5. In the case of wind speed, the correlations between the AWS data and LDAPS were  $0.27 \text{ m s}^{-1}$  in summer and  $0.46 \text{ m s}^{-1}$  in winter. Regardless of the season, the air temperature showed a high correlation of 0.8 or more.

In the Rm type, 18 AWS points were selected. The average Bias of each point for wind speed and temperature was 0.48 and 0.82, similar to the results of 25 points analyzed above. The larger difference between the LDAPS terrain altitude and actual terrain altitude, the lower prediction performance of LDAPS. The correlation between two data on wind speed was 0.28, which showed the lowest correlation among the four categories, and the correlation with temperature was 0.83, showing a high correlation similar to other categories.

In the case of the Rc type, where 15 points were selected, the wind speed was overestimated at all points as in the analysis in the previous

section. In case of wind speed, the average of Bias at 15 points was 2.40, which showed the largest deviation from the observed values among the four categories. This is the result of the characteristics of LDAPS, which regards the small islands, which are the characteristics of the Rc type shown above, as the sea. In the case of air temperature, the average of Bias at 15 points was very small, 0.09, but the deviation was 0.4, a different prediction characteristic appeared at each point. The correlations between AWS data and LDAPS were 0.40 in winter and 0.24 in summer, in case of wind speed, and the case of air temperature was 0.82 in summer and 0.57 in winter.

The characteristics of the LDAPS prediction at the additional selected point were numerically different from those shown in Section 3.2, but the prediction characteristics by the land cover and topography were similarly.

Station number	Difference of altitude	type	Bias (wind speeds/temperature)	R <sup>2</sup> (wind speeds/temperature)	Station number	Difference of altitude	type	Bias (wind speeds/temperature)	R <sup>2</sup> (wind speeds/temperature)
96	96.18	Rc	2.96 / 0.66	0.19 / 0.78	625	-61.75	Rm	1.57 / -0.03	0.35 / 0.83
303	97.87	Rc	3.97 / 0.37	0.13 / 0.80	628	31.89	Rf	0.19 / 0.16	0.43 / 0.92
311	-246.51	Rm	2.15 / -0.06	0.24 / 0.74	634	27.15	Rf	1.26 / -0.10	0.46 / 0.80
312	89.97	Rm	1.16 / -0.33	0.45 / 0.87	641	-69.96	Rf	1.16 / -0.27	0.28 / 0.88
314	706.84	Rm	-1.11 / 3.90	0.01 / 0.80	642	21.24	Uf	0.63 / -0.59	0.46 / 0.92
317	-291.80	Rf	1.57 / -1.30	0.30 / 0.80	643	-35.29	Uf	1.21 / -0.36	0.35 / 0.86
325	-65.72	Rf	0.40 / -0.09	0.45 / 0.87	654	10.49	Rc	3.46 / -0.09	0.27 / 0.75
327	56.82	Rf	1.15 / 0.43	0.37 / 0.85	659	567.95	Rm	-0.87 / 3.08	0.04 / 0.79
328	-39.18	Rf	1.48 / -0.64	0.52 / 0.80	665	22.88	Rc	2.51 / 0.43	0.33 / 0.72
497	-140.76	Rm	2.65 / 0.31	0.33 / 0.71	670	-45.29	Rf	0.96 / -0.50	0.33 / 0.79
498	206.34	Rm	0.38 / 1.35	0.23 / 0.88	673	3.90	Rf	0.28 / 0.31	0.48 / 0.91
499	-46.71	Rf	0.78 / 0.34	0.34 / 0.90	680	-169.95	Rm	0.72 / -0.66	0.20 / 0.85
502	13.97	Rc	1.66 / -0.05	0.33 / 0.81	692	-52.11	Rf	0.53 / 0.49	0.33 / 0.97
506	1.85	Uf	0.40 / 0.39	0.42 / 0.92	693	-42.22	Uf	0.74 / -0.54	0.42 / 0.93
511	34.01	Rf	1.04 / -0.08	0.41 / 0.89	694	419.93	Rm	-2.05 / 2.90	0.25 / 0.80
516	-7.99	Rf	0.24 / 0.18	0.40 / 0.92	702	3.63	Uf	0.72 / 0.25	0.33 / 0.90
520	117.60	Rf	1.13 / -0.03	0.32 / 0.66	703	5.10	Rf	0.50 / 0.50	0.31 / 0.89
531	-220.69	Rf	0.81 / -0.62	0.25 / 0.79	716	5.15	Rc	1.30 / -0.68	0.57 / 0.75
536	-118.95	Rf	0.59 / -0.48	0.32 / 0.89	717	-19.53	Rf	1.06 / -0.04	0.30 / 0.87
537	-141.66	Rm	1.20 / -0.57	0.43 / 0.84	725	9.26	Rc	2.44 / -0.09	0.53 / 0.69
538	-39.22	Rf	0.20 / 0.05	0.20 / 0.89	734	-1.35	Rf	0.14 / 0.16	0.29 / 0.89
540	5.55	Rf	0.99 / 0.48	0.48 / 0.90	738	8.32	Rf	0.27 / 0.13	0.53 / 0.89
541	-70.43	Uf	0.84 / -0.15	0.37 / 0.90	743	8.23	Rc	1.72 / -0.66	0.57 / 0.74
543	25.82	Rc	1.95 / -0.22	0.28 / 0.71	747	26.03	Rc	3.28 / -0.17	0.21 / 0.67
546	-72.80	Rf	0.73 / -0.48	0.19 / 0.92	750	34.90	Rc	1.08 / 0.04	0.45 / 0.81
548	33.96	Uf	0.71 / -0.31	0.31 / 0.76	752	49.65	Rf	0.42 / 0.45	0.44 / 0.88
549	-50.30	Uf	0.71 / -0.31	0.31 / 0.91	754	-21.10	Rf	1.10 / -0.71	0.48 / 0.90
550	9.90	Rf	0.70 / -0.01	0.49 / 0.93	757	-159.41	Rm	0.85 / 0.09	0.29 / 0.84
551	27.58	Uf	0.40 / -0.12	0.44 / 0.94	777	-31.31	Rf	0.06 / -0.78	0.47 / 0.88
555	-78.47	Rf	0.50 / 0.23	0.27 / 0.86	812	-21.15	Rf	0.80 / 0.76	0.28 / 0.87
556	-183.22	Uf	0.45 / -0.53	0.28 / 0.94	822	-135.22	Rf	0.75 / -0.37	0.36 / 0.81
557	-24.59	Rm	0.48 / -0.03	0.40 / 0.88	823	-30.13	Rf	0.33 / 0.71	0.45 / 0.87
562	-47.66	Rf	-0.19 / 0.08	0.41 / 0.89	827	2.65	Rf	0.88 / -1.03	0.25 / 0.90
565	-1.53	Rf	0.62 / -0.33	0.49 / 0.87	828	24.23	Rc	3.23 / 0.38	0.04 / 0.85
568	-125.66	Uf	0.71 / -0.44	0.28 / 0.84	841	-51.91	Rf	0.31 / 0.42	0.41 / 0.82
569	-25.82	Uf	0.64 / -0.47	0.32 / 0.92	846	1.38	Uf	0.53 / -0.69	0.36 / 0.93
570	6.75	Uf	0.97 / -0.24	0.36 / 0.90	854	-3.85	Rf	0.80 / 0.06	0.31 / 0.91
575	2.38	Rf	0.69 / 0.41	0.46 / 0.88	859	55.31	Rm	1.64 / -0.06	0.31 / 0.89
580	-129.84	Rf	0.10 / -0.85	0.29 / 0.79	860	24.73	Uf	0.38 / -0.13	0.32 / 0.80
588	-91.70	Rf	0.50 / 0.17	0.40 / 0.83	871	371.10	Rm	0.15 / 2.44	0.37 / 0.73
590	-209.69	Uf	1.34 / -1.58	0.32 / 0.79	873	351.48	Rm	-1.48 / 2.13	0.11 / 0.86
591	9.79	Rm	0.56 / 0.27	0.27 / 0.86	885	-124.20	Rf	-0.06 / 0.15	0.33 / 0.77
595	-69.85	Rm	0.08 / -0.01	0.41 / 0.79	905	-210.96	Rf	0.61 / -0.87	0.31 / 0.81
598	-41.28	Uf	0.55 / 0.32	0.29 / 0.87	908	-154.35	Rf	0.76 / -0.25	0.36 / 0.74
600	16.72	Rf	0.59 / 0.22	0.40 / 0.88	909	111.49	Rc	1.71 / 0.73	0.21 / 0.77
601	-42.59	Uf	0.63 / -0.57	0.29 / 0.91	913	-37.82	Rf	0.37 / -0.43	0.24 / 0.83
604	3.18	Rf	0.76 / -0.44	0.46 / 0.92	918	-2.91	Rf	-0.42 / 0.39	0.30 / 0.89
609	36.13	Rc	2.13 / 0.24	0.38 / 0.72	927	-137.60	Rf	0.46 / -0.19	0.42 / 0.84
610	16.91	Rc	2.63 / 0.41	0.32 / 0.62	932	-23.10	Rf	0.76 / -0.78	0.22 / 0.92
622	-50.61	Rm	0.60 / 0.03	0.46 / 0.84	939	-127.74	Uf	0.85 / -0.60	0.29 / 0.82

**Table 3. Information of additional 100 AWS points.**

## 4. Summary & Conclusions

In this study, the Characteristics of wind Speed and air temperature predicted by the local data assimilation of prediction system (LDAPS) for different land covers and topographies were analyzed. AWS sites were classified into four categories according to land cover and topography and compared with wind speed and air temperature predictions at the nearest LDAPS grid point. For the Uf type, due to the limitation of the resolution that LDAPS, it does not properly reflect the influence of the flow disturbance by the building and the heating effect due to the land cover. As the results, the average wind speed was  $0.96 \text{ m s}^{-1}$  overestimated and the average air temperature was  $0.97^{\circ}\text{C}$  underestimated. In case of Rf type, wind speed and air temperature were  $0.55 \text{ m s}^{-1}$  overestimation, and  $0.16^{\circ}\text{C}$  underestimation, respectively. Because of few obstacles around the observation point, the LDAPS prediction performance was higher than the Uf type. The performance of LDAPS prediction for Rm type was significantly influenced by the difference between the LDAPS topographic altitude and the actual terrain altitude. At the AWS points where the LDAPS terrain altitude is expressed to be lower than the actual altitude were underestimated the wind speed and overestimated the temperature. At the AWS points where the

LDAPS terrain altitude is higher than the actual altitude, the opposite pattern appeared. The Rc type has different prediction characteristics when the LDAPS grids were located on land or sea. When the LDAPS grid was represented by the sea, LDAPS was overestimated in wind speed much more in comparison with AWS observations data. In the case of air temperature, overall underestimation was observed, but no significant correlation was observed between the each points.

In the flat terrain, the prediction characteristics of LDAPS are different depending on the building and covering conditions around the observation point, which can be improved by coupling with the model which can consider the detailed topography like computational fluid dynamics (CFD) model. In addition, the LDAPS characteristic that shows a large deviation by the terrain is expected to be able to improve the prediction performance by improvement of the resolution or the parameterization of the terrain elevation and the ground state such as the urban parameterization.

## REFERENCES

- Best, M.J., 2005. REPRESENTING URBAN AREAS WITHIN OPERATIONAL NUMERICAL WEATHER PREDICTION MODELS, *Boundary-Layer Meteorology*, 114, 91-109.
- Kang, M.S., Y.-K. Lim, C.B. Cho, K.R. Kim, J.S. Park, and B.-J. Kim, 2015. The Sensitivity Analyses of Initial Condition and Data Assimilation for a Fog Event using the Mesoscale Meteorological Model. *Journal of Korean Earth Science*, 36(6), 567-579.
- Kim, D.Y., T.W. Kim, G.J. Oh, J.C. Huh, and K.N. Ko, 2016. A comparison of ground-based LiDAR and met mast wind measurements for wind resource assessment over various terrain conditions. *Journal of Wind Engineering and Industrial Aerodynamics*, 158, 109-121.
- Kwon, Y.-A., H.-Y. Lee, 2003. The Characteristics of Air Temperature Distribution by Land-use Type – A case study of around Automatic Weather Station in Seoul, *Journal of environmental impact assessment*, 12(4), 291-290.
- Lee, D. B., and H.-Y. Chun, 2015. Development of the Korean Peninsula-Korean Aviation Turbulence Guidance (KP-KTG) System Using the Local Data

Assimilation and Prediction System (LDAPS) of the Korea Meteorological Administration (KMA). *Atmosphere*, 25(2), 367-374.

Lee, J.W., and Y.S. Kim, 2007. Coastline Change Analysis Using RTK-GPS and Aerial Photo, *Journal of the Korean Society of Surveying*, 25(3), 191-198.

Lesk, C., P. Rowhani, and N. Ramankutty, 2016. Influence of extreme weather disasters on global crop production. *Nature*, 529(7584), 84.

Lim, E.-H., I.-H. Cho, J.-O. Lim, and Y.-H. Park, 2011. Establishment of local prediction system based on unified model, *KMA*, 2011-02.

Park, S.-J., S.-H. Choi, J.-E. K, D.-J. Kim, D.-S. Mun, W.S. Choi, J.-J. Kim, and Y.-G. L, 2016. Effects of Differential Heating by Land-Use types on flow and air temperature in an urban area. *Korean Journal of Remote Sensing*, 32(6), 603-616.

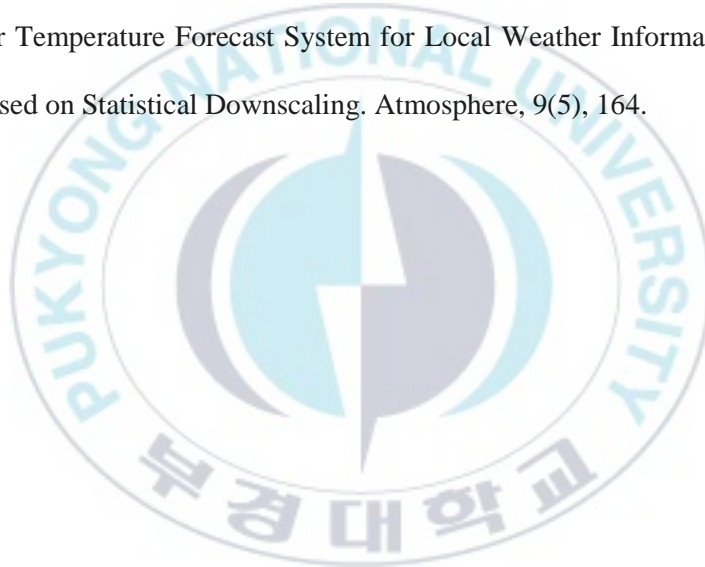
Park. S. -U., I.-H. Lee, S.J. Joo, and J.-W. Ju, 2017. Emergency preparedness for the accidental release of radionuclides from the Uljin Nuclear Power Plant in Korea, *Journal of Environmental Radioactivity*, 180, 90-105.

Song, B. H., 2014. A Case Study of the Meteorological Industry for the Media in the USA for Promotion of Private Sector Meteorological Industry in the

Republic of Korea: Based on The Weather Channel Case. *Atmosphere*, 24(2), 253-263.

Sung, C. -J., 2003. A Study on the Analysis of Terrain Element and Terrain Classification Using GIS, *The Geographical Journal of Korea*. 37(2), 155-161.

Yi, C., Shin, Y., and Roh, J. W., 2018. Development of an Urban High-Resolution Air Temperature Forecast System for Local Weather Information Services Based on Statistical Downscaling. *Atmosphere*, 9(5), 164.



## 감사의 글

2016년 10월, 도시대기연구실에 들어온 지 2년하고도 6개월가량 지나 어느덧 졸업을 앞두고 있는 순간까지 학문과 외적으로 큰 도움을 주신 많은 분들께 이 작은 지면을 빌어 짧게나마 감사의 마음을 전하고자 합니다.

가장 먼저, 제가 학부생이던 시절부터 2016년 진흥원에서 일하며 석사학위에 대해 진지하게 고민할 때, 그리고 2년이란 석사 과정 동안 늘 학생의 입장에서 먼저 생각해주시고 학문적인 가르침 이외에도 고난과 역경의 시간을 이겨낼 수 있는 버팀목이 되어주신 김재진 교수님께 감사드립니다. 교수님의 훌륭한 가르침을 바탕으로 대한민국의 기상학을 한층 더 발전시켜 ‘역시 김재진 교수님’ 이라는 말이 나오도록 최선을 다하겠습니다. 그리고 이제는 은퇴하신 변희룡 교수님, 오재호 교수님, 옥곤 교수님과 여전히 존경스러운 모습으로 강단에 서시는 이동인 교수님, 정형빈 교수님, 권병혁 교수님의 훌륭한 가르침에 깊은 감사의 인사를 드립니다. 또한, 공동 지도교수로 늘 가까운 곳에서 많은 가르침을 주신 최원식 교수님과 미흡했던 석사 학위 발표와 논문을 한층 더 높은 수준으로 끌어올릴 수 있도록 지도해주신 김백민 교수님께 감사의 말씀을 드립니다.

2년이 넘는 시간을 동거동락하며 정말 많은 가르침을 주고 권위의식 없이 연구실 식구들을 정말 가족처럼 대해준 도시대기연구실의 수호신 박수진 선배님께 감사 드립니다. 그리고, 석사 과정을 시작하기까지 많은 고민이 있을 때, 그리고 2년이란 시간 동안 큰 힘이 되어주고 때론 선배로써 많은 가르침과 도움을 주고, 때론 친구로써 힘든 시간을 이겨나갈 수 있게 해준 장운이와 건이에게 감사 드립니다. 연구실에 들어오기 전까지는 가까운 사이도 아니었으며, 학번 차이도 많이 나는 선배라

상대하기 어려웠을 텐데 거리낌없이 대해주고 연구실에서는 선배이자 졸업 동기로 마지막까지 힘들 때나 지칠 때 ‘석삼 파이팅’을 외치며 힘이 되어주고 짓궂은 장난까지 받아주며 즐겁게 연구실 생활을 마무리 할 수 있게 도와준 다숨이와 정은이에게 감사 드립니다. 그리고 비록 같이 생활하지 않았지만 각지에서 연구적으로나 생활적으로도 큰 힘이 되어 주신 연구실 사형들께 감사 드립니다.

석사과정 동안 수많은 투덜거림과 징징거림을 받아주고 학사관리에 필요한 부분들을 챙겨준 선배이자 조교선생님이자 형이자 친구로 늘 큰 힘이 되어준 김원호 씨와 내가 지칠 때마다 김원호 조교를 데리고 사라져 홀로 일 처리를 하느라 고생하면서도 많은 내색은 하지 않고 결국 이 힘든 시간을 이겨낼 수 있게 해준 김은영 전 조교님께도 감사 드립니다.

4호관 3층에서 만난 인연들과 모든 사람의 이름을 언급하지는 못하지만 학부생 시절부터 지금에 이르기까지 늘 힘이 되어주고 격려를 아끼지 않은 내 친구들에게 큰 감사를 드립니다.

마지막으로 이 글을 쓰고 있는지도 모를 내 가장 소중한 가족 여러분께 감사 드립니다. 직장을 그만두고 타지에서 대학원을 진학한다고 했을 때, 내키지 않았지만 저의 결정을 존중해주시고 항상 믿음을 주신 부모님의 훌륭한 가르침과 지원 덕에 빼어나진 않지만 훌륭한 사람이 되었습니다. 그리고 솔직히 큰 도움은 안됐지만 존재만으로도 힘이 된 형과 동생에게 두줄 짜리 감사의 인사를 드립니다.

다시 한 번 글로는 다 표현하지 못할 감사한 마음을 전합니다. 감사합니다.